

1996

A Microstructural Investigation of Calcium Hydroxyapatites Synthesized from $\text{CaHPO}_4 \cdot 2\text{H}_2\text{O}$ and $\text{Ca}_4(\text{PO}_4)_2\text{O}$

Kevor S. TenHuisen
Corporate Biomaterials Center

Boyd A. Clark
The Pennsylvania State University

Maria Klimkiewicz
The Pennsylvania State University

Paul W. Brown
The Pennsylvania State University

Follow this and additional works at: <https://digitalcommons.usu.edu/cellsandmaterials>

 Part of the [Biomedical Engineering and Bioengineering Commons](#)

Recommended Citation

TenHuisen, Kevor S.; Clark, Boyd A.; Klimkiewicz, Maria; and Brown, Paul W. (1996) "A Microstructural Investigation of Calcium Hydroxyapatites Synthesized from $\text{CaHPO}_4 \cdot 2\text{H}_2\text{O}$ and $\text{Ca}_4(\text{PO}_4)_2\text{O}$," *Cells and Materials*: Vol. 6 : No. 1 , Article 24.

Available at: <https://digitalcommons.usu.edu/cellsandmaterials/vol6/iss1/24>

This Article is brought to you for free and open access by the Western Dairy Center at DigitalCommons@USU. It has been accepted for inclusion in Cells and Materials by an authorized administrator of DigitalCommons@USU. For more information, please contact digitalcommons@usu.edu.



A MICROSTRUCTURAL INVESTIGATION OF CALCIUM HYDROXYAPATITES SYNTHESIZED FROM $\text{CaHPO}_4 \cdot 2\text{H}_2\text{O}$ AND $\text{Ca}_4(\text{PO}_4)_2\text{O}$

Kevor S. TenHuisen, Boyd A. Clark^{1,2}, Maria Klimkiewicz¹ and Paul W. Brown^{1,*}

Johnson and Johnson, Corporate Biomaterials Center, P.O. Box 151, Somerville, NJ 08876-0151

¹The Pennsylvania State University, Materials Research Laboratory, University Park, PA 16802

²R.J. Lee Group, Inc., 350 Hochberg Road, Monroeville, PA 15146

(Received for publication March 25, 1996 and in revised form November 4, 1996)

Abstract

This investigation determined the effects of reaction temperature and bulk composition on the microstructural features of hydroxyapatites (HAp) synthesized from reaction between particulate $\text{CaHPO}_4 \cdot 2\text{H}_2\text{O}$ and $\text{Ca}_4(\text{PO}_4)_2\text{O}$. These data were used in combination with previous work to further elucidate the mechanistic reaction path taken by these calcium phosphate cements. HAp's having two different compositions ($\text{Ca}/\text{P} = 1.50$ and 1.67) were synthesized between 15.0 and 70.0°C. All reactions reached completion as indicated by X-ray diffraction. Single point nitrogen absorption was performed on all samples to determine specific surface areas. The HAp which is approximately stoichiometric ($\text{Ca}/\text{P} = 1.67$) had a surface area equal or greater than that of calcium-deficient HAp ($\text{Ca}/\text{P} = 1.50$) synthesized at the same temperature. All surface areas were equal to or greater than those typically reported for bone and were in accord with average crystallite sizes as determined by dark field transmission electron microscopy (TEM) for all but one sample. Observations using scanning electron microscopy support previous X-ray diffraction studies and indicate the reactivity of $\text{Ca}_4(\text{PO}_4)_2\text{O}$ limited the rate of HAp formation. Electron diffraction by TEM verified the presence of very small proportions of an electron amorphous phase. The proportion of this phase increased with a decrease in reaction temperature, and it was more prevalent in the calcium-deficient HAp. Two distinct morphologies, plates and nodules, were observed by TEM. The nodules contained more amorphous material, while the plates were determined to have the c-axis approximately perpendicular to the plate face.

Key Words: Calcium phosphate cements, brushite, tetracalcium phosphate, hydroxyapatite, microstructure, transmission electron microscopy, scanning electron microscopy, surface area.

*Address for Correspondence:

Paul W. Brown, address as above.

Telephone: (814) 865-5352 / FAX: (814) 863-7040

Introduction

Calcium phosphate cements (CPCs) are a relatively new class of materials that have many possible applications in dentistry and orthopaedics. These cements have numerous advantages over materials presently used. CPCs can be formulated to have initial consistencies that range from an injectable fluid to a stiff paste. This property would allow a high degree of flexibility during implantation. Upon reaction, CPCs will harden into monoliths that effectively fill complex voids and bond both mechanically and eventually chemically to native hard tissue. It has been demonstrated that *in vivo* placement of calcium phosphate cement induces minimal adverse tissue reactions in endodontic procedures in monkeys (Hong *et al.*, 1991) and craniofacial studies on cats (Costantino *et al.*, 1992; Friedman *et al.*, 1991). These studies have also demonstrated that normal anatomic contours were maintained with new bone formation at the progressive implant-bone interface.

Another advantage of CPCs is the inherent flexibility of their chemistry and kinetics. There are a number of calcium phosphates, when combined in the proper stoichiometries, that can react together or hydrolyze separately at physiologic temperature to form monolithic hydroxyapatite $\{\text{HAp}, \text{Ca}_{10-x}(\text{HPO}_4)_x(\text{PO}_4)_{6-x}(\text{OH})_{2-x}\}$. These include:

- (1) monocalcium phosphate monohydrate, MCPM $\{\text{Ca}(\text{H}_2\text{PO}_4)_2 \cdot \text{H}_2\text{O}\}$;
- (2) brushite or DCPD $\{\text{CaHPO}_4 \cdot 2\text{H}_2\text{O}\}$;
- (3) monetite or DCP $\{\text{CaHPO}_4\}$;
- (4) octacalcium phosphate or OCP $\{\text{Ca}_8(\text{HPO}_4)_2(\text{PO}_4)_4 \cdot 5\text{H}_2\text{O}\}$;
- (5) α -tricalcium phosphate or α -TCP $\{\text{Ca}_3(\text{PO}_4)_2\}$;
- and (6) tetracalcium phosphate or TetCP $\{\text{Ca}_4(\text{PO}_4)_2\text{O}\}$.

These compounds are typically characterized by their Ca/P molar ratios. HAp does not have a fixed composition; rather, it exists over a range of Ca/P ratios. While Ca/P ratios between ~ 1.33 and 1.67 have been reported (Heughebaert *et al.*, 1990; Nancollas, 1989; Zawacki *et al.*, 1990) for precipitated HAp in the $\text{CaO}-\text{P}_2\text{O}_5-\text{H}_2\text{O}$ ternary system, the lowest Ca/P ratio

achieved for a calcium phosphate cement that reacts to completion to form HAp is 1.50 (Brown, 1992; Martin and Brown, 1994, 1997; TenHuisen *et al.*, 1995).

Compositional variability, combined with the ability of apatites to substitute a variety of cations and anions into their structure, allows a high degree of flexibility in tailoring the chemistry and kinetics of the cement formation and properties of the resultant product. Variability in composition greatly affects the solubility and the microstructure of HAp. Both the solubility of the apatite and its microstructure ultimately influence the rate of ingrowth and resorption that would occur *in vivo*. Decreasing the Ca/P ratio from 1.67 to 1.50 in the absence of substituents increases the solubility of the HAp (TenHuisen and Brown, 1997; Zawacki *et al.*, 1990). It has been shown that the incorporation of carbonate increases the solubility of HAp due to the distortion of the lattice (Nelson *et al.*, 1989). Alternatively, fluoride substitution decreases the apatite solubility as reflected in a smaller solubility product and extends its stability range to lower pH values (Chin and Nancollas, 1991; Moreno *et al.*, 1974, 1977). Another important factor to consider is the effect of surface area on the apparent solubility. High surface areas usually result in higher apparent solubilities due to higher initial dissolution rates and surface effects.

Extensive electron microscopy studies have been performed on biological apatites (Brès *et al.*, 1990, 1993; Daculsi *et al.*, 1984; Jackson *et al.*, 1978; Nakahara and Kakei, 1984) and synthetic apatites (Iijima *et al.*, 1992a, 1992b; Meyer *et al.*, 1972; Nelson *et al.*, 1986), investigating morphology, crystallite orientation, and lattice parameters and defects. To date, an in depth investigation of the microstructural features of HAp formed by CPC reactions has not been performed. In the present study, we have investigated the microstructure and surface area of HAp formed by reacting DCPD and TetCP as a function of reaction temperature and Ca/P ratio. Such investigation is intended to give insight into the ways HAp formed by these types of reactions might interact *in vivo*. Understanding the mechanistic reaction paths taken is also essential to tailoring these cements for *in vivo* use. Determining changes in microstructure and surface area assists in establishing these mechanisms.

Materials and Methods

TetCP and DCPD synthesis

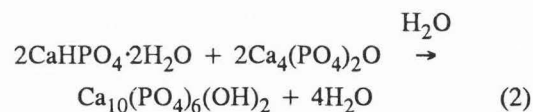
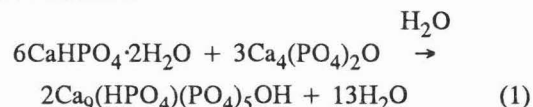
TetCP was synthesized by a high temperature solid state reaction between reagent grade monetite (CaHPO_4 ; Fisher Scientific, Pittsburgh, PA) and precipitated calcium carbonate (CaCO_3 , Fisher). Equimolar quantities of monetite and calcium carbonate were homogenized by milling and then fired at 1400°C for two hours.

The fired product was ground by hand and then milled to a particle size of $\sim 2.5 \mu\text{m}$ as determined by light scattering particle size analysis. X-ray diffraction was used to confirm phase purity. No evidence of hydroxyapatite or lime (CaO) was observed.

DCPD (300 g) was precipitated via an acid-base reaction between calcium hydroxide and monocalcium phosphate monohydrate (MCPM, $\text{Ca}(\text{H}_2\text{PO}_4)_2 \cdot \text{H}_2\text{O}$). To prepare calcium hydroxide, precipitated calcium carbonate (Fisher) was calcined at 1100°C for two hours to CaO and then ground in a mortar and pestle. A calcium hydroxide slurry was prepared by the addition of 48.435 g of CaO to 750 ml of deionized water in a sealed 1 liter Nalgene bottle (obtained from Fisher Scientific, Pittsburgh, PA). This slurry was added to a slurry of 217.71 g of reagent grade MCPM (J.T. Baker, Phillipsburg, NJ) in 2250 ml of deionized water. The suspension was stirred for 15 minutes and then filtered through #5 Whatman (Springfield Mill, UK) filter paper. The precipitate was dispersed in acetone (2500 ml) and again filtered to remove excess water. The precipitate was dried under vacuum ($\sim 4 \times 10^{-2}$ torr) using a cold trap to capture the acetone. X-ray diffraction confirmed phase pure DCPD. No HAp was present on the surfaces of the DCPD as observed by scanning electron microscopy (SEM).

HAp Synthesis

DCPD and TetCP powders were combined in 2-to-1 and 1-to-1 molar ratios and milled together to constitute initial mixtures with Ca/P molar ratios of 1.50 and 1.67. Reactions 1 and 2 show the formation of calcium-deficient HAp (Ca/P = 1.50, CDHAp) and HAp which is approximately stoichiometric (Ca/P = 1.67, SHAp) from these reactants.



The reactant powders were reacted with deionized water at a liquid-to-solids weight ratio of 1-to-1 within an isothermal calorimeter to monitor the evolution of heat as a function of reaction time (TenHuisen and Brown, 1996). Reactions were performed at the following temperatures: 15, 20, 25, 30, 33.5, 37.4, 40, 45, 50, 55, 60, 65, and 70°C . The reactant powder and deionized water were separately equilibrated to each reaction temperature before reaction initiation. Upon reaching thermal equilibrium, the water was injected onto the powder. After complete reaction was reached, as indicated by the absence of further heat evolution, the

samples were frozen in liquid nitrogen and freeze-dried to remove excess water.

Characterization

All samples were characterized by X-ray diffraction and surface area analysis. Powder X-ray diffraction indicated complete reaction to HAp occurred for both stoichiometries at all reaction temperatures. A Scintag powder diffractometer (PAD V, Scintag Inc., Sunnyvale, CA) with $\text{CuK}\alpha$ radiation was utilized. All samples were scanned over a two theta (2θ) range of 10° - 35° at a rate of 2° 2θ per minute with a step size of 0.02° . Selected samples were scanned over a 2θ range of 3° - 35° to check for the presence of octacalcium phosphate (OCP).

Single point nitrogen absorption (Monosorb MS-12, Quantachrome Corp., Syosset, NY) was used to determine the surface areas of the HAp. All samples were dried at 150°C overnight prior to outgassing for 45 minutes at 150°C . A 30/70 mixture of N_2/He was used. All samples were run in triplicate, and their values averaged. The values of each triplicate were all within $\pm 1 \text{ m}^2/\text{g}$ of one another.

Selected samples were observed in a scanning electron microscope (ISI-DS 130; Topcon Technologies, Paramas, NJ). Sample were coated with gold. Scanning electron photomicrographs were obtained in the secondary electron image mode.

Samples observed by SEM were also observed in a transmission electron microscope (TEM; JEOL 2000, JEOL Ltd., Tokyo, Japan). Samples were ground in anhydrous methanol and sonicated for approximately 60 seconds. These suspensions were filtered through $0.2 \mu\text{m}$ polycarbonate membranes and then coated with carbon. The polycarbonate membranes were dissolved in chloroform, and the carbon film containing the samples were placed onto copper grids for TEM observation. The camera constant was determined using the first five diffraction rings from a gold standard.

Results and Discussion

Surface area

Figure 1 plots surface areas of SHAp and CDHAp as a function of reaction temperature. The surface areas recorded are relatively high and range between ~ 75 - $165 \text{ m}^2/\text{g}$. These surface areas are in the range of values reported for deproteinized bone (Misra *et al.*, 1978). A prior calorimetric study of these systems indicated HAp formed from DCPD and TetCP by a nucleation and growth mechanism (TenHuisen and Brown, 1996). The large change in surface area with reaction temperature is consistent with the high temperature dependence observed for the kinetics of these reactions.

The surface areas vary with temperature, showing

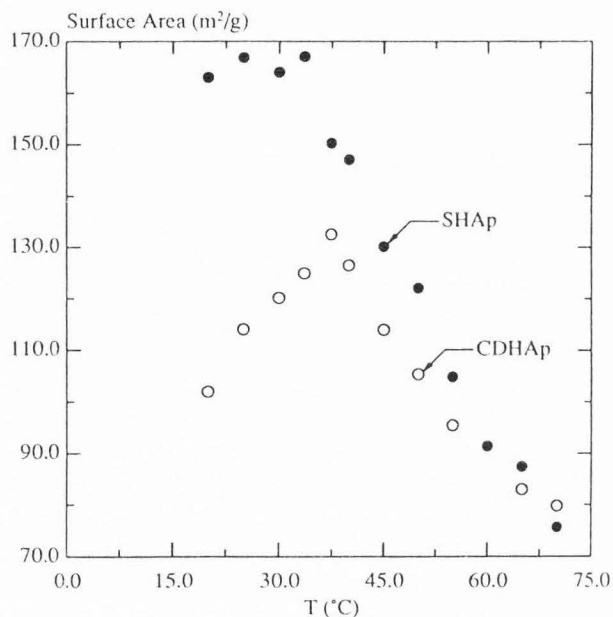


Figure 1. Surface areas of CDHAp and SHAp formed from DCPD and TetCP plotted as a function of reaction temperature.

two trends with a transition occurring at approximately physiologic temperature. In the higher temperature range (~ 35 to 70°C), the surface areas for SHAp and CDHAp decrease with increasing temperature. SHAp formed at 33.5°C attains the maximum surface area observed ($\sim 165 \text{ m}^2/\text{g}$); CDHAp attains a maximum of $\sim 130 \text{ m}^2/\text{g}$ at 37.4°C . Reductions in surface areas with increasing temperature in this range indicate a decrease in the nucleation/growth rate ratio (i.e., the ratio of the nucleation rate to growth rate) even though the overall rate of HAp formation rapidly increases with increasing temperature. At the elevated reaction temperatures (55° to 70°C), there are only small differences between the surface areas of the two compositions. This is due to the extremely high rate of HAp formation which reaches completion within 0.5 hour for CDHAp and SHAp at 70°C (TenHuisen and Brown, 1996).

At temperatures close to physiologic, SHAp displays increasingly greater surface areas compared to CDHAp. SHAp formation occurs at pH values higher than CDHAp (TenHuisen and Brown, 1997; Zawacki *et al.*, 1990). Previous work has also shown that an intermediate noncrystalline calcium phosphate phase (NCP) precipitates in DCPD-TetCP reactions which subsequently transforms to apatite (TenHuisen and Brown, 1997). A greater nucleation density at higher pH values should occur in the calcium phosphate system because the solubilities of both NCP and SHAp decreases as the pH rises, thus resulting in a higher degree of supersaturation

and nucleation density. Others (Blumenthal and Posner, 1972) have reported an increase in the surface area with increasing pH for NCP formation, supporting the present observations. The relative proportion of the NCP intermediate formed in DCPD-TetCP reactions is independent of reaction temperature for a given bulk composition (TenHuisen and Brown, 1996), and only very small quantities of it were observed by TEM (discussed subsequently) upon complete reaction. Therefore, the measured surface area results from the crystalline HAp; the NCP has a negligible contribution.

Very different surface area trends occur at reaction temperatures below physiologic for the two HAp compositions. SHAp maintains a relatively constant surface area of $\sim 165 \text{ m}^2/\text{g}$ below 37.4°C , independent of the reaction temperature. Therefore, the nucleation/growth rate ratio must remain nominally constant between 15° and 37.4°C , although the overall rate of SHAp formation continuously decreases with decreasing temperature. After reaching a maximum in surface area at physiologic temperature, the surface area of CDHAp decreases with decreasing temperature. This indicates the nucleation/growth rate ratio must then decrease with decreasing temperature.

The differences in CDHAp and SHAp surface areas at temperatures below physiologic is also related to the relatively larger proportion of DCPD in the initial reactant mixture with $\text{Ca}/\text{P} = 1.50$. It has been shown that reactions involving DCPD and TetCP form a noncrystalline calcium phosphate intermediate (TenHuisen and Brown, 1997); electron microscopy and electron diffraction evidence for this will be discussed in a later section. Relatively more of the NCP intermediate is formed when the initial $\text{Ca}/\text{P} = 1.50$. The proportion of this phase was observed to be independent of the reaction temperature for a given bulk stoichiometry (TenHuisen and Brown, 1996, 1997). Thus, the trend observed in the surface area is likely related to the HAp that forms from the transformation of this larger proportion of NCP intermediate. As the reaction temperature is decreased, the NCP transforms to HAp (Boskey and Posner, 1973) more slowly, resulting in larger apatite crystals.

Scanning electron microscopy

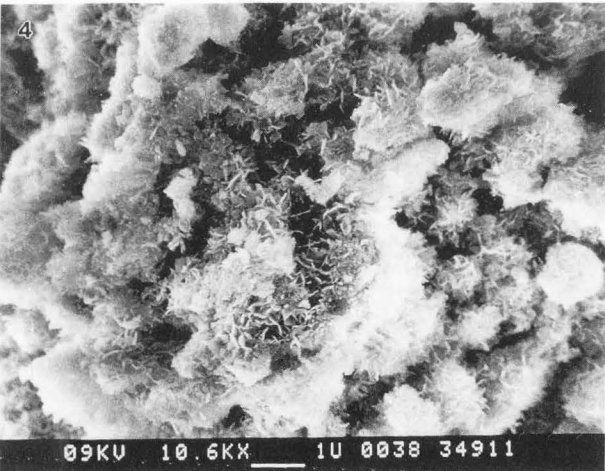
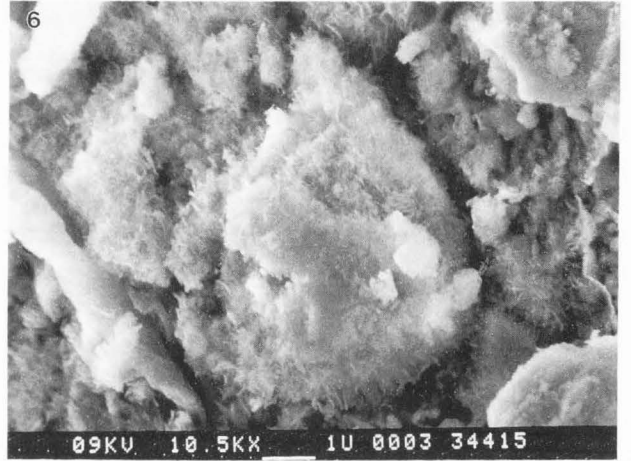
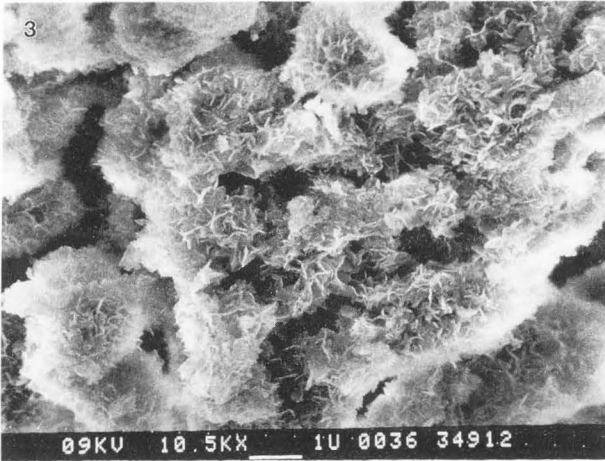
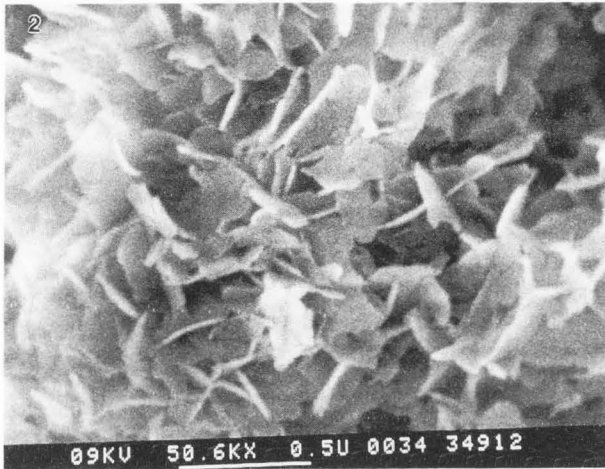
SEM investigations were performed on samples synthesized at the maximum and minimum reaction temperatures of this study (15° and 70°C) and at the transition temperatures dividing the two surface area trends (37.4°C for CDHAp and 33.5°C for SHAp). Figures 2-4 compare the SEM microstructures of CDHAp and SHAp formed at 70°C . The microstructural features of the two samples are quite similar and characterized by irregularly shaped thin plates (see Fig. 2). These plates appear to be less than $\sim 50 \text{ nm}$ in thickness and less

than $\sim 400 \text{ nm}$ across. The great similarity in microstructure correlates with similar kinetics of formation (TenHuisen and Brown, 1996) and almost identical surface areas.

The spatial relationship between the initial reactant particles and the HAp formed can be seen at lower magnifications (Figs. 3 and 4). Pseudomorphs of the initial TetCP appear as irregularly shaped spheres composed of multiple plates. These spheres are connected to one another via interparticulate precipitates. This interparticulate connectivity is lowest at the elevated reaction temperatures. This finding suggests that the reactions forming the HAp occur in close apposition to the TetCP surfaces, resulting in less precipitation of HAp between TetCP particles. This finding supports pH values observed as a function of reaction temperature, time, and stoichiometry (TenHuisen and Brown, 1997). The steady-state pH values during reaction decreased with increasing temperature, suggesting that the TetCP becomes overgrown more rapidly as the reaction temperature increases. This is likely due to the retrograde solubility of SHAp (McDowell *et al.*, 1977) and the epitaxial relationship between TetCP and HAp (Dickens and Schroeder, 1980).

In general, the microstructural features become more irregular as the reaction temperature is decreased. Figures 5 and 6 show microstructures typical of SHAp (33.5°C) and CDHAp (37.4°C), respectively. SHAp shows prominent differences compared to that formed at 70°C . The plate-like features apparent at 70°C have become more interconnected with one another and ribbon-like. They also appear to be smaller than the plates formed at 70°C . Overall, the microstructure appears more interconnected. A prominent feature in this sample is the presence of shell structures or "donuts." This microstructural feature is more prevalent in SHAp and increases as the reaction temperature decreases. These donuts result from the overgrowth of TetCP with HAp, resulting in the consumption of TetCP from the inside of the particles. This observation supports previous findings showing that TetCP is the rate limiting reactant (TenHuisen and Brown, 1997). The presence of shells and finer features result in an increase in the surface area as previously discussed.

CDHAp formed at 37.4°C also shows large changes in its microstructural features from that formed at 70.0°C . Not only is it more irregular, the features are much finer (see Fig. 6). The overall morphology shows complete integration of the initial reactant particles into a structure that is highly interconnected. The pseudomorphs of the TetCP particles are coated with very fine needles and plates, resulting in the maximum surface area for this composition. The interparticulate connectivity appears to reach a maximum at this temperature

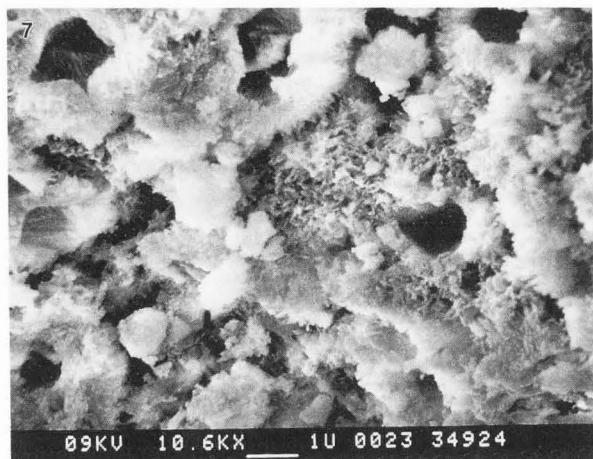


Figures 2-6. Representative microstructures of: **Figure 2.** CDHAp and SHAp formed at 70°C characterized by distorted hexagonal plates. **Figure 3.** SHAp formed at 70°C showing the platy microstructure and the relationship between the initial precursor particles and formed HAp. **Figure 4.** Microstructure of CDHAp formed at 70°C showing the platy microstructure and the relationship between the initial precursor particles and formed HAp. **Figure 5.** Microstructure of SHAp formed at 33.5°C illustrating a more interconnected structure than at 70°C and the appearance of shell structures or "donuts." **Figure 6.** Microstructure of CDHAp formed at 37.4°C showing a high degree of interparticulate bonding and finer features than reaction at 70°C. Bars = 0.5 μm (Fig. 2) and 1 μm (Fig. 3-6).

for the CDHAp. Few donut-like features occur in this sample due to the lower proportion of the rate limiting reactant, TetCP.

SHAp formed at 15°C exhibits a maximum in interparticulate connectivity (see Fig. 7). This is evident as

ribbon-like plates and needles formed between the artifacts of the TetCP particles. Shells or donuts are prevalent again as a result of the overgrowth of the rate limiting reactant, TetCP. The most discernible microstructural differences are the features present at the interiors



Figures 7-9. Microstructures (formed at 15°C) of: **Figure 7.** SHAp showing a maximum in interparticulate connectivity for this composition and a high frequency of "donuts." **Figure 8.** SHAp showing the fine features present within the remnants of the TetCP particles. **Figure 9.** CDHAp; the interparticulate connectivity appears less than that occurring in samples formed at 37.4°C and the features are not as fine. Bars = 1 μ m.

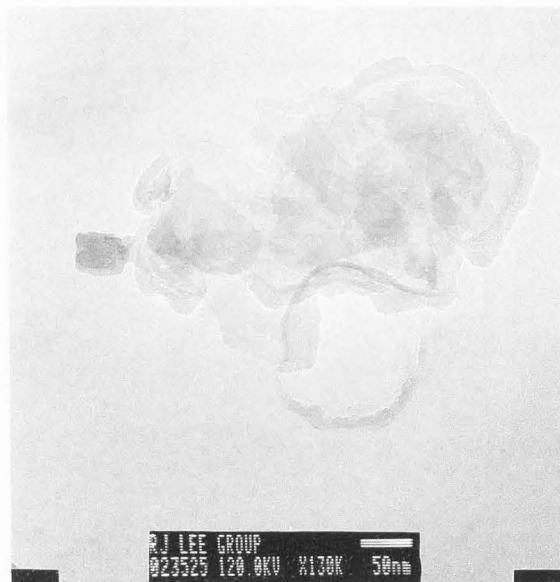


Figure 10. Representative platey morphology observed in all samples. Bar = 50 nm.

of the shells. Extremely fine needles showing preferred alignment occur (Fig. 8). This alignment results from slow epitaxial growth of HAp on the TetCP surface.

The characteristic microstructure of CDHAp formed at 15°C is shown in Figure 9. There is again a high degree of interconnectivity, although it appears to be slightly less than that at 37.4°C. The structural features are not as fine as those in the 37.4°C sample. Although not shown in Figure 9, shells also become apparent in the CDHAp and occur due to the slower kinetics of the system resulting in some overgrowth of the TetCP. In comparing the microstructures of CDHAp and SHAp formed at 15°C, it is difficult to explain the large difference in surface area. The most significant difference is the greater frequency of shells present in SHAp. Thus, the additional area may result from this inner surface and the extremely small crystallites observed.

Transmission electron microscopy

Samples imaged by SEM were also observed by TEM. Three primary microstructural features were observed: plates, needles, and nodules (see Figs. 10-12). These structural features were observed at both stoichiometries over the entire temperature range of this study. As shown in Figure 10, the plates are extremely thin. Preliminary observation suggested that needles were present in the samples (Fig. 11). For example, Figure 13 shows what appears to be a needle. Plates are also apparent in the background. Upon tilting this location by 40°, the true morphology, a plate on edge, was revealed (Fig. 14). Thus, the three apparent microstructural features illustrated in Figures 10-12 are actually

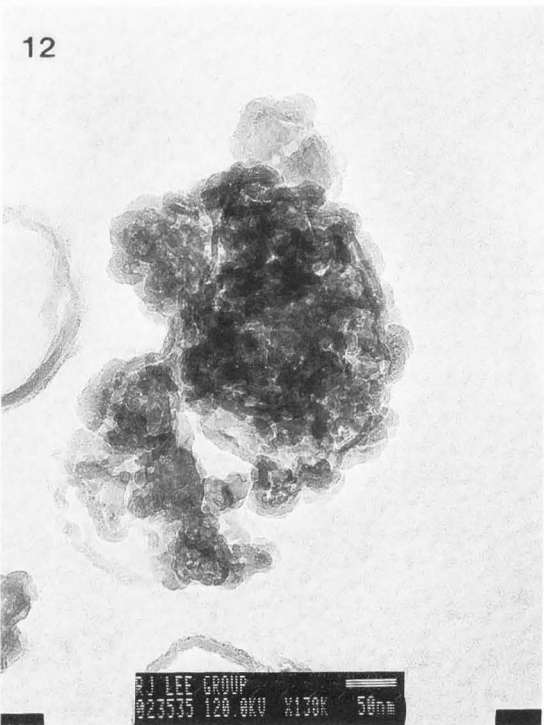
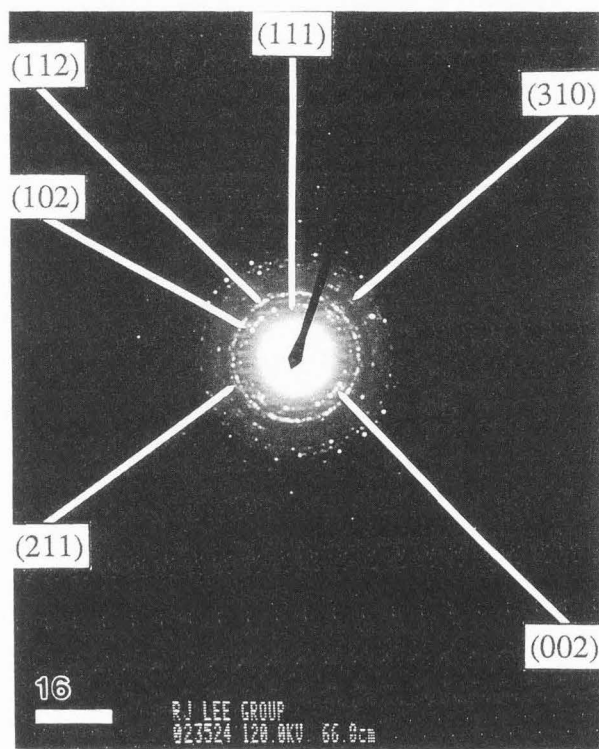
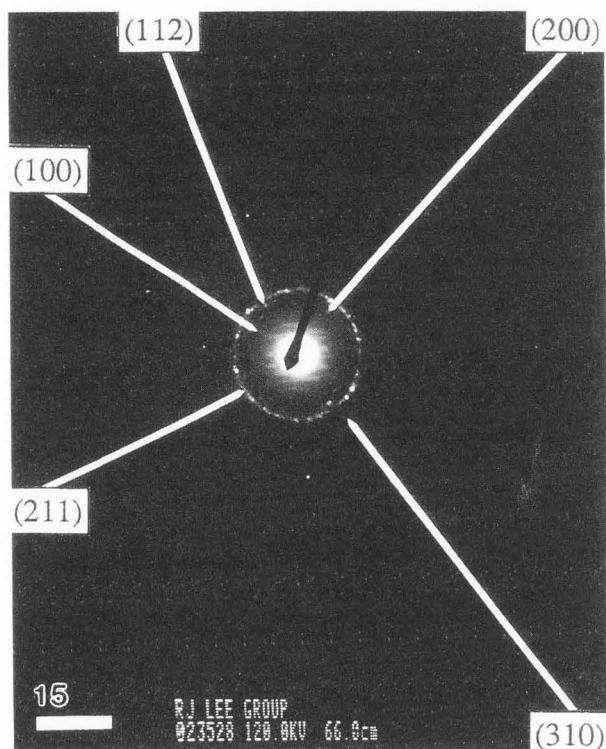


Figure 11. Representative needle morphology observed in all samples. This morphology was later shown to result from plates on edge. Bar = 50 nm.

Figure 12. Representative nodular morphology observed in all samples and characterized by ribbon-like and spherical features. Bar = 50 nm.

Figure 13. Microstructure at 0° tilt showing what was originally believed to be needles. Bar = 50 nm.

Figure 14. Microstructure at 40° tilt showing that needles are actually plates-on-edge. Bar = 50 nm.



Figures 15 and 16. Electron diffraction pattern of a plate-on-edge (Fig. 15) and a plate-on-flat (Fig. 16). The camera constant is 23.50 mm-Å. Bar = 1 cm.

only two: plates (and plates-on-edge) and nodules. The thicknesses of these plates range between ~ 2 and 15 nm (Fig. 11). The plates were more prevalent as the reaction temperature increased. This suggests that higher temperatures favor a more defined plate-like structure, even though the overall kinetics are much faster.

An analysis of diffraction patterns from plates-on-edge compared to plates-on-flat was performed. The analysis confirmed the structure to be pseudo-hexagonal as given by JCPDS card 9-432 (Joint Committee on Powder Diffraction Standards, Philadelphia, 1967). It was observed that only certain planes diffracted when the plates were on edge (Fig. 15) compared to plates-on-flat (Fig. 16) as shown in the diffraction patterns in Figures 15 and 16. This preliminary analysis indicates that the *c*-axis of the perpendicular of the flat plate.

Figure 12 shows the second morphological feature observed in the HAP samples. These nodules are irregular and poorly defined, but appear to be composed of small agglomerates, ribbon-like features, and possibly small plates. Electron diffraction was performed on regions where the plates and nodules formed separately. The diffraction rings of the nodules appear much more diffuse than those of the plates. This suggests that the platey regions are more crystalline. The appearance of lower "crystallinity" in the nodules can be attributed

to one of two factors: the presence of a second amorphous phase and/or much smaller crystallites.

The nodular regions showed a lower crystalline content by dark field imaging. This is consistent with the presence of a nondiffracting or noncrystalline phase. While X-ray diffraction is not the most sensitive technique for detecting amorphous phases in the presence of nanocrystalline material, previous work (TenHuisen and Brown, 1997) has indicated the presence of an amorphous phase as an intermediate of these reactions. In the precipitation of HAP from neutral salts, intermediate compounds, such as amorphous calcium phosphate (ACP) and OCP, can form. The precipitation of these intermediates depends on the solution conditions, i.e., supersaturation, pH, and extraneous ions.

In this study, TEM verified the presence of a completely electron amorphous phase (see Fig. 17) with a morphology typical of ACP1 (Christoffersen *et al.*, 1990). The morphology of ACP1 is characterized by spherical plates and that of ACP2 by an acicular structure; neither produces an electron diffraction pattern. Figure 18 is the electron diffraction pattern of the ACP1 shown in Figure 17 and shows the absence of any diffraction resulting from a crystalline material. The faint diffuse rings observed in Figure 17 result from the carbon support and is a preparative artifact.

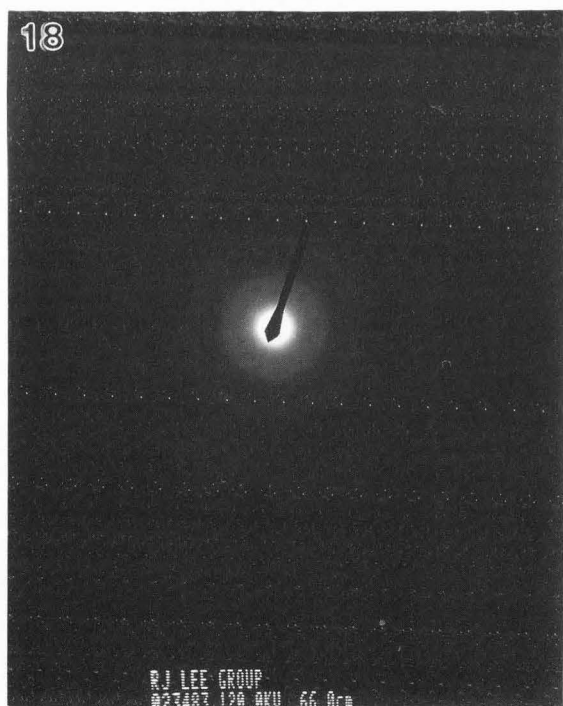
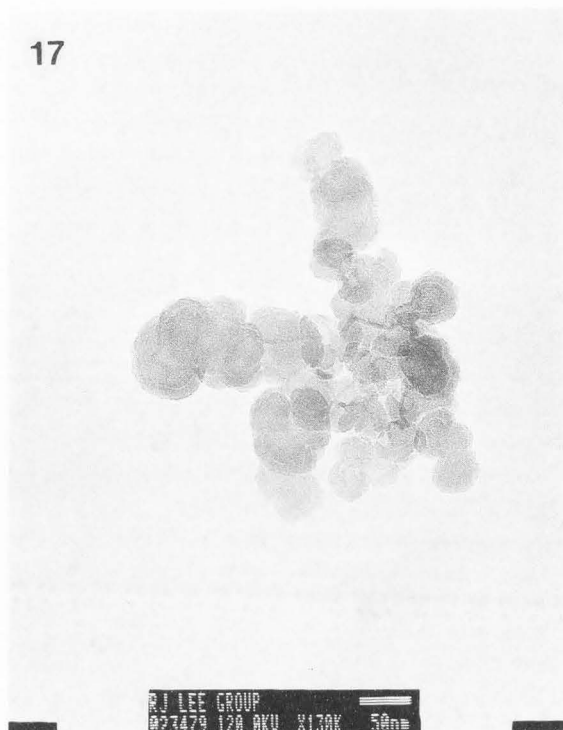


Figure 17. Representative microstructural evidence for the presence of an amorphous calcium phosphate phase observe in all samples. The flat spherical morphology of this electron amorphous phase is characteristic of ACP. Bar = 50 nm.

Figure 18. Electron diffraction pattern of ACP shown in Figure 17. The faint diffuse rings result from the carbon used during sample preparation.

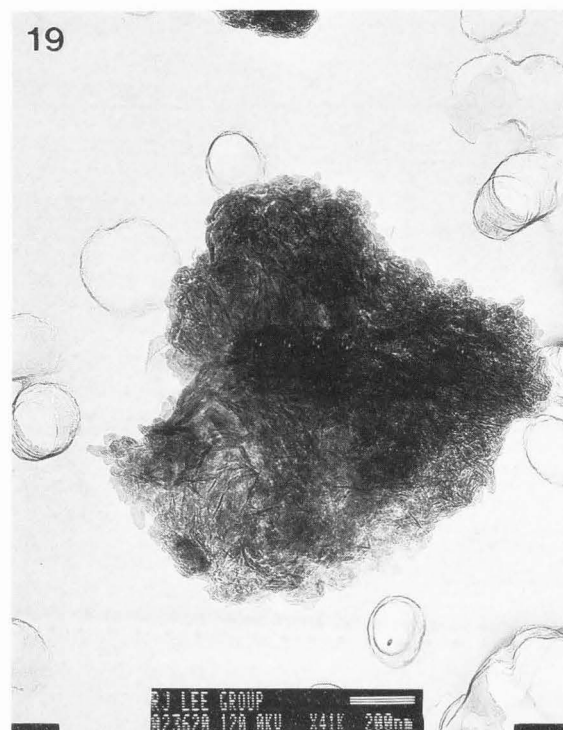


Figure 19. Representative microstructure illustrating the morphology of regions characterized by intermixed nodules and plates. This morphology is characteristic of that resulting from the conversion of ACP to HAp. Bar = 200 nm.

In many areas of the samples, the nodular structure was intermixed with plates (Fig. 19). The structure shown in Figure 19 is very similar to the microstructure observed when ACP is converted to HAp (Eanes and Meyer, 1977). This is further microstructural evidence of the formation of amorphous intermediates from DCPD-TetCP reactions. Although observed in all samples, the proportion of this amorphous phase was quite small in comparison to that of HAp, and its presence resulted from the reaction being quenched slightly before completion. Aging these apatites in their mother liquor for extended times resulted in the disappearance of this intermediate phase.

Although statistical analyses were not performed, visual observations indicate the nodular and ACP morphologies were more prevalent at lower reaction temperatures and in CDHAp. The higher stability of ACP with decreasing temperature and previous calorimetric (TenHuisen and Brown, 1996) and solution chemistry (TenHuisen and Brown, 1997) data on this system are in accord with these TEM observations. The pH range in which CDHAp (Ca/P = 1.50) forms (TenHuisen and Brown, 1997) indicates that the HAp forming during the initial part of the reaction has a Ca/P > 1.50 (Zawacki

Table 1. Crystallite sizes as a function of stoichiometry and temperature.

Temperature (°C)	Bulk Ca/P ratio	Average Crystallite Size (nm)	Range of Crystallite Sizes (nm)
70.0	1.67	35	5-47
70.0	1.50	48	4-100
37.4	1.67	24	4-44
37.4	1.50	23	2-47
15.0	1.67	23	4-53
15.0	1.50	24	4-52

et al., 1990). This, in combination with the preferential dissolution of the acidic reactant, DCPD, indicates that a secondary phase, with a Ca/P < 1.50 must be present. Because OCP was not observed, formation of an NCP with a Ca/P < 1.50 would be expected and should be more prevalent in the CDHAp samples.

Table 1 shows the distribution of crystallite sizes observed in each sample. To determine the crystallite size, dark field images of each sample were examined and the size of the diffracting crystallites measured. Representative dark field images used for crystallite size determinations are shown in Figures 20 and 21. Because only the features diffracting electrons at a chosen position will be highlighted in a dark field image, the feature must be crystalline, be oriented in a particular manner, and be a single phase. These analyses are qualitative in nature. The number of crystallites is quite large, and only a limited number of crystallites were measured (approximately 50 crystallites for each sample at each temperature). The dark field data indicate a larger crystallite size for CDHAp and SHAp formed at the highest temperature (70°C) as compared to the lower reaction temperatures. This agrees with the surface area data (Fig. 1) previously discussed in that CDHAp and SHAp show the lowest surface areas when formed at 70°C. The crystallite sizes are approximately the same for both CDHAp and SHAp formed at 37.4° (CDHAp)/33.5° (SHAp) and 15.0°C. This is also consistent with surface area trends for the SHAp sample; the surface area is both constant over the temperature range of 33.5 to 15.0°C and larger than for reaction at 70°C. Based on the surface area measurements a larger crystallite size would be expected for CDHAp formed at 15.0°C than at 37.4°C. However, there is a complex relationship between crystallite size and surface area for CDHAp

which is complicated by the formation of the NCP intermediate, its subsequent conversion to HAp, and the complex microstructure of the apatitic product. The fine crystallite sizes observed by TEM at 37.4° (CDHAp), 33.5° (SHAp), and 15°C (SHAp) are consistent with the structures observed by SEM previously discussed.

Conclusions

Particulate DCPD and TetCP mixed at Ca/P molar ratios of 1.50 and 1.67 reacted to completion to form CDHAp and SHAp, respectively, at all temperatures investigated. Small proportions of a noncrystalline calcium phosphate phase were observed by TEM and verified by electron diffraction. Although present in small amounts, the proportion of NCP was observed to increase with decreasing temperature and was more prevalent in CDHAp. These findings are consistent with previous calorimetric and solution chemistry data indicating its formation and eventual conversion to apatite. Two predominant morphological features were observed by TEM, plates and nodules. Analysis of the plate orientation indicates the c-axis to be approximately perpendicular to the plate surface. Dark field imaging indicated dimensions of the crystallites to be on the order of those in bone and that the nodular regions were "less crystalline" than the platey regions. SEM analysis showed a general increase in microstructural regularity and decrease in interparticulate connectivity with increasing temperature. These observations in part result from the retrograde solubility of HAp and partial overgrowth of the TetCP particles. The observations of an increasing number of "shells" or "donuts" with decreasing temperature and their higher frequency in the SHAp support earlier findings that TetCP is the rate limiting reactant when DCPD and TetCP react to form HAp. The surface areas of the HAp formed could be related to its average crystallite size, the exception being the CDHAp sample formed at 15.0°C.

The results of this study indicate that the rates of HAp formation will be most affected by varying the TetCP particle size. Although present in small proportions, the verification of presence of a NCP phase supports the proposed mechanism for reaction between DCPD and TetCP in which a NCP intermediate phase is formed. Both CDHAp and SHAp had surface areas equivalent to or greater than those typically observed in deproteinated bone. Forming HAp at near physiologic temperature with high surface areas should facilitate resorption *in vivo* provided the macroporosity is properly tailored. The high degree of interparticulate connectivity that occurs near physiologic temperature indicates that the mechanical properties of these cements can be optimized at these temperatures.

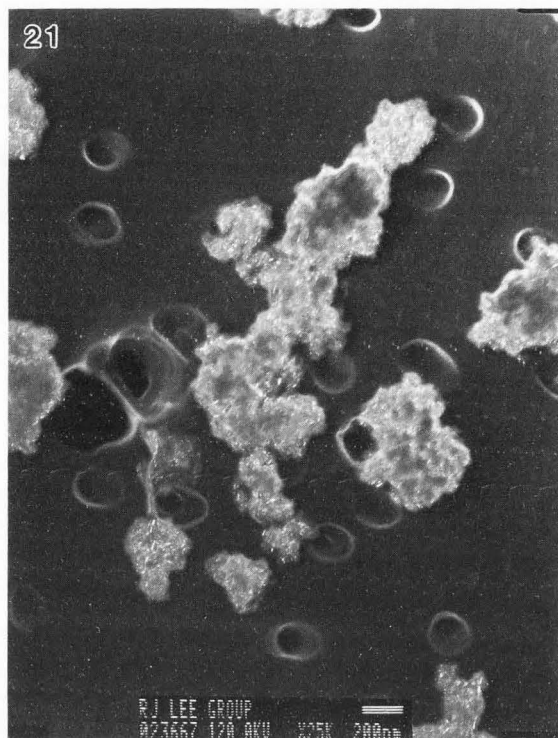
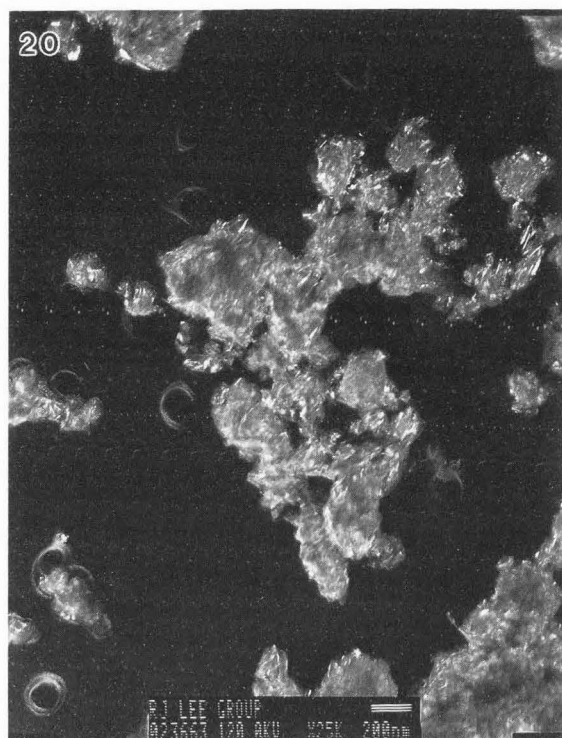


Figure 20 and 21. Representative dark field images for CDHAp used to determine the average crystallite size of HAp formed at 37.4°C (**Fig. 20**) and at 70°C (**Fig. 21**). Note the significant increase in crystallite size at 70°C compared to CDHAp formed at 37.4°C. Bars = 200 nm.

Acknowledgment

The authors acknowledge the National Institutes of Health, Grant #DE09421, for financial support.

References

Blumenthal NC, Posner AS (1972) Effect of preparation conditions on the properties and transformation of amorphous calcium phosphate. *Mater Res Bull* **7**: 1181-1190.

Boskey AL, Posner AS (1973) Conversion of amorphous calcium phosphate to microcrystalline hydroxyapatite. A pH-dependent, solution-mediated, solid-solid conversion. *J Phys Chem* **77**: 2313-2317.

Brès EF, Voegel JC, Frank RM (1990) High resolution electron microscopy of human enamel crystals. *J Microscopy* **160**: 183-201.

Brès EF, Steuer P, Voegel JC, Frank RM, Cuisinier FJG (1993) Observation of the loss of the hydroxyapatite sixfold symmetry in a human fetal tooth enamel crystal. *J Microscopy* **170**: 147-154.

Brown PW (1992) Phase relationships in the ternary

system CaO-P₂O₅-H₂O. *J Am Ceram Soc* **75**: 17-22.

Chin KOA, Nancollas GH (1991) Dissolution of fluorapatite. A constant-composition kinetics study. *Langmuir* **7**: 2175-2179.

Chow LC (1991) Development of self-setting calcium phosphate cements. *J Ceram Soc Japan* **99**: 954-964.

Christoffersen MR, Christoffersen J, Kibalczyk W (1990) Apparent solubilities of two amorphous calcium phosphates and of octacalcium phosphate in the temperature range 30-42°C. *J Cryst Growth* **106**: 349-354.

Costantino PD, Friedman CD, Jones K, Chow LC, Sisson GA (1992) Experimental hydroxyapatite cement cranioplasty. *Plastic Reconstruct Surg* **90**: 174-191.

Daculsi G, Menanteau J, Kerebel LM, Mitre D (1984) Length and shape of enamel crystals. *Calcif Tissue Res* **36**: 550-555.

Dickens B, Schroeder LW (1980) Investigation of epitaxy relationships between Ca₅(PO₄)₃OH and other calcium ortho-phosphates. *J Res Natl Bur Stand* **85**: 347-362.

Eanes ED, Meyer JL (1977) The maturation of crystalline calcium phosphates in aqueous suspensions at physiological pH. *Calcif Tissue Res* **23**: 259-269.

Eidelman N, Chow LC, Brown WE (1987) Calcium phosphate phase transformations in serum. *Calcif Tissue Int* **41**: 18-26.

Friedman CD, Costantino PD, Jones K, Chow LC, Pelzer HJ, Sisson GA Sr (1991) Hydroxyapatite cement. II. Obliteration and reconstruction of the cat frontal sinus. *Arch Otolaryng -- Head Neck Surg* **117**: 385-389.

Heughebaert JC, Zawacki SJ, Nancollas GH (1990) The growth of nonstoichiometric apatite from aqueous solution at 37°C. I. Methodology and growth at pH 7.4. *J Colloid Interf Sci* **135**: 21-32.

Hong YC, Wang JT, Hong CY, Brown WE, Chow LC (1991) The periapical tissue reactions to a calcium phosphate cement in the teeth of monkeys. *J Biomed Mater Res* **25**: 485-498.

Iijima M, Tohda H, Moriwaki Y (1992a) Growth and lamellar mixed crystals of octacalcium phosphate and apatite in a model system of enamel formation. *J Cryst Growth* **116**: 319-326.

Iijima M, Tohda H, Suzuki H, Yanagisawa T, Moriwaki Y (1992b) Effects of F⁻ on apatite-octacalcium phosphate intergrowth and crystal morphology in a model system of tooth enamel formation. *Calcif Tissue Int* **50**: 357-361.

Jackson SA, Cartwright AG, Lewis D (1978) The morphology of bone mineral crystals. *Calcif Tissue Res* **25**: 217-222.

Levin EM, McMurdie HF (1975) Phase Diagrams for Ceramists. Vol. III. The American Ceramic Society, Westerville, OH. p. 15, 17.

Levin EM, Robbins CR, McMurdie HF (1964) Phase Diagrams for Ceramists. Vol. I. The American Ceramic Society, Columbus, OH. p. 38.

Martin RI, Brown PW (1994) Formation of hydroxyapatite in serum. *J Mater Sci: Mater Med* **5**: 96-102.

Martin RI, Brown PW (1995) Mechanical properties of hydroxyapatite formed at 38°C. *J Mater Sci: Mater Med* **6**: 138-143.

Martin RI, Brown PW (1997) Aqueous formation of hydroxyapatite. *J Biomed Mater Res*, **35**: 299-308.

McDowell H, Moreno TM, Brown WE (1977) Solubility of Ca₅(PO₄)₃OH in the system Ca(OH)₂-P₂O₅-H₂O at 5, 15, 25, and 37°C. *J Res Natl Bur Stand* **81A**: 273-281.

Meyer JL, Eick JD, Nancollas GH, Johnson LN (1972) A scanning electron microscopic study of the growth of hydroxyapatite crystals. *Calcif Tissue Res* **10**: 91-102.

Misra DN, Bowen RL, Matamal GJ (1978) Surface area of dental enamel, bone, and hydroxyapatite: Chemisorption from solution. *Calcif Tissue Res* **26**: 139-142.

Moreno EC, Kresak M, Zahradnik RT (1974) Fluoridated hydroxyapatite solubility and caries formation. *Nature* **247**: 64-65.

Moreno EC, Kresak M, Zahradnik RT (1977) Physicochemical aspects of fluoride-apatite systems relevant to the study of dental caries. *Caries Res* **11** (suppl. 1): 142-160.

Nakahara H, Kakei M (1984) TEM observations on the crystallites of dentin. *Bull Josai Dent Univ* **13**: 259-263.

Nancollas GH (1989) In vitro studies of calcium phosphate crystallization. In: *Biomaterialization, Chemical and Biochemical Perspectives*. Mann S, Webb J, Williams RJP (eds.). VCH Publishers, Weinheim, Germany. pp. 157-187.

Nelson DGA, Wood GJ, Barry JC, Featherstone JDB (1986) The structure of (100) defects in carbonated apatite crystallites: A high resolution electron microscope study. *Ultramicroscopy* **19**: 253-266.

Nelson DGA, Barry JC, Shield CP, Glens R, Featherstone JDB (1989) Crystal morphology, composition and dissolution behavior of carbonated apatites prepared under controlled pH and temperature. *J Colloid Interf Sci* **130**: 467-479.

Taylor HFW (1990) *Cement Chemistry*. Academic Press, NY. p. 146-154.

TenHuisen KS, Martin RI, Klimkiewicz M, Brown PW (1995) Formation and properties of a synthetic bone composite: Hydroxyapatite-collagen. *J Biomed Mater Res* **29**: 803-810.

TenHuisen KS, Brown PW (1996) The kinetics of calcium deficient and stoichiometric hydroxyapatite formation from CaHPO₄·2H₂O and Ca₄(PO₄)₂. *J Mater Sci: Mater Med* **7**: 309-316.

TenHuisen KS, Brown PW (1997) Variations in solution chemistry during calcium-deficient and stoichiometric hydroxyapatite formation from CaHPO₄·2H₂O and Ca₄(PO₄)₂. *J Biomed Mater Res*, in press.

Zawacki SJ, Heughebaert JC, Nancollas GH (1990) The growth of nonstoichiometric apatite from aqueous solution at 37°C. II. Effects of pH upon the precipitated phase. *J Colloid Interf Sci* **135**: 33-44.

Discussion with Reviewers

G. Daculsi: How is SEM able to demonstrate that no HAp was present in the DCPD that you synthesized in the **Materials and Methods** section? Morphological data are not enough.

Authors: SEM was used in combination with X-ray diffraction. X-ray diffraction has a sensitivity, at best, of ~2% by weight. When HAp is present in combination with DCPD, it can be observed by SEM as a surface phase on the DCPD crystals. It can be observed long before it can be detected by either wet chemical analysis techniques or by diffraction techniques. The pH of the final solution also indicates that only DCPD should be

present, as it was below the invariant point pH between DCPD and HAp. Therefore, SEM was used as a complimentary technique in determining the phase purity of this reactant.

G. Daculsi: The final apatites were scanned over a 2θ range of 10° to 35° , this is too limited. A 2θ range of 10 to 45° would be better. Please comment.

P. Li: X-ray diffraction data of the starting materials and the resultant products should be given in the paper with the scanning range extending at least to 2θ of 40° because they are important to understand the cementing reaction and the microstructure of the resultant products.

D.G.A. Nelson: The sample were scanned over a range that was too narrow (10° to 35°). This misses a strong OCP peak at 1.84 nm at around 4° - 5° (2θ). A more suitable range should go out to 50° - 60° (2θ). The presence of other phases might have been missed.

E. Brès: How do the authors know that no OCP but an NCP is formed?

Authors: While a 2θ range of 10° to 35° is limited, all of the major calcium phosphate reflections occur over this range. Scanning out to 45° does not assist in identifying any additional calcium phosphate phases in the present system. If we were determining lattice parameters, a larger scan range would have been necessary, but we were only interested in phase identification in this study. We did scan selected samples (those prepared below 50°C) down to 3° to determine if any OCP was present. Upon complete reaction, only the reflections resulting from HAp were observed. There also was no evidence by electron diffraction of the 1.84 nm reflection characteristic of OCP. Evidence for NCP is shown in Figures 17-19 and discussed in the text.

G. Daculsi: Have you performed tests on the kinetics of dissolution in buffer and/or physiologic fluid?

Authors: We have not performed any such tests on the final apatite formed by these reactions. Our immediate goal was to obtain a better understanding of the reaction path taken by these CPCs. Our group has investigated the effects of calf serum and albumin on the reaction path taken during HAp formation from DCP (CaHPO_4) and TetCP (Martin and Brown, 1994). Eidelman *et al.* (1987) have also investigated the phase transformations and solution conditions of various calcium phosphate phases in serum.

G. Daculsi: Have you determined the compressive strength of the material obtained?

Authors: Not in the present study. Our group has shown that these types of reactions result in compressive strengths equal to those obtained from HAp synthesized by high temperature techniques at equal porosities

(Martin and Brown PW, 1995). L.C. Chow has also reported compressive strength values for CPCs ranging between 34 MPa and 51 MPa (Chow, 1991).

G. Daculsi: The work published in Science {Constantz BR, Ison IC, Fulmer MT, Posner RD, Smith ST, Van-Wagoner M, Ross J, Goldstein SA, Jupiter JB, Rosenthal DI (1995) Skeletal repair by *in situ* formation of the mineral phase of bone. Science 267: 1796-1799} on CPCs (SRS Norian, Cupertino, CA) was not cited. Can you comment on the differences?

Authors: While Norian's SRS product is a calcium phosphate cement, the formation reaction is quite different than the CPC discussed in the present work. The SRS cement formulation is more complex than DCPD-TetCP. According to the Science paper, SRS contains CaCO_3 , MCPM [$\text{Ca}(\text{H}_2\text{PO}_4)_2 \cdot 2\text{H}_2\text{O}$], and α -TCP [$\text{Ca}_3(\text{PO}_4)_2$] which are dry mixed prior to the addition of a sodium phosphate solution. Thus, different reactants are used. Differences in the kinetics and the mechanistic paths taken in the two systems appear to depend on the selection of reactants. NCP formation accompanies reaction of DCPD and TetCP whereas formation of DCPD as an intermediate undoubtedly accompanies the hydrolysis of MCPM.

D.G.A. Nelson: The decrease in surface area at low temperatures for CDHAp samples is explained by the presence of an amorphous precursor phase. Would not an amorphous phase have a very high surface area? Are there no other explanations for these results (agglomerates, sampling errors, electron beam amorphization, etc.)?

Authors: While our microscopy study indicates NCP formation, the quantity of this intermediate remaining upon complete reaction is relatively small. Its main contribution to the surface area results from differences in the surface area of HAp formed from its conversion in comparison to the apatite directly precipitated from the two reactant calcium phosphate powders. This, of course, may not be the only reason for the observations in surface area made in this investigation, but it is a plausible explanation for the results observed. Sampling error should be minimal as the samples were run in triplicate; all values were within $\pm 1 \text{ m}^2/\text{g}$ of one another. Electron beam amorphization is irrelevant because the samples were measured prior to imaging. Agglomeration and pore structure could affect the measured surface area, but only if closed pores are present in the samples. At this time, we do not know the degree of closed porosity in our samples, or if this changes with composition and reaction temperature.

D.G.A. Nelson: What size of field-limiting aperture

was used for the electron diffraction patterns?

Authors: The aperture size was 20 μm . Due to the dispersion of the particles, the diffraction aperture could be offset so as not to pick up diffracted beams from unwanted crystallites/orientations. Only the diffracted beams from the crystallites of the desired orientation were in the field.

D.G.A. Nelson: Even though the diffraction pattern looks more diffuse for the nodules, spots and rings were still observed indicating the presence of crystalline material with a smaller fundamental particle size (i.e., coherently diffracting domains) than the reference material. What evidence is there that an amorphous phase exists?

Authors: The absence of a complete, well-defined diffraction ring and the observation that not all material can be made to "light-up" in dark-field imaging (regardless of sample orientation) are evidence of an amorphous phase. There could well be sub-angstrom sized coherent domains present in the material, but this level of order is approaching that of an amorphous material.

D.G.A. Nelson: What diffracted beams were used in the dark-field imaging? The dark-field imaging process only uses a few of the diffracted beams in the imaging process. Thus, not all crystallographic domains will "light-up" in a dark-field image such as those shown in Figures 20 and 21, only those in the correct orientation. Also crystal thickness can affect the contrast of a diffracting domain. The images do not verify the existence of an amorphous phase. They are precisely what is observed for an agglomerate of small crystallites.

Authors: Figures 20 and 21 were shown to illustrate the size of the individual crystals. The exact diffracted beams for these are unknown, but for our study this is not an issue. If any diffracted beam is used for the dark-field images, entire crystals with that particular orientation will "light-up." By moving the aperture from diffracted beam to diffracted beam, one can qualitatively ascertain how much of the material is amorphous or crystalline. As the diffracted beam is varied, we see some areas of the sample "light-up," indicating crystalline regions, while other areas never "light-up," indicating they are electron amorphous.

E. Brès: Does the TEM sample preparation used (grinding in anhydrous methanol and dissolution in chloroform) damage the samples? Would it not be simpler to use water and to let the sample dry?

Authors: One must always be concerned about the effects of preparation technique on the sample. The samples were suspended in alcohol in order to obtain a better dispersion of the particles. The problem with using

water as a medium, and especially evaporation for its removal, is that the sample agglomerates making dispersion of the particles difficult if not impossible. The effect of grinding on the sample would be more likely to alter the sample than short exposures to alcohol or chloroform. It has been shown that grinding and milling can result in localized temperatures that are hundreds of degrees higher than that of the surrounding. At worst, these liquids would remove residual free water in the system. The presence of anhydrous polar solvents has been shown to have negligible effects on calcium phosphates such as OCP [$\text{Ca}_8(\text{HPO}_4)_2(\text{PO}_4)_6 \cdot 5\text{H}_2\text{O}$], DCPD, and amorphous calcium phosphate when used for rinsing/removal of residual free water. The ideal preparative technique would involve no solvents, chemical etchants, mechanical energy, or ion milling. This of course is impractical for almost all samples.

E. Brès: As for the orientation of the crystal planes with respect to the crystal faces, the best approach would be to make a single diffraction pattern of a crystal oriented along the [0001] axis and compare it to an image of the same crystal. The arguments put forward by the authors are weak since planes at an angle to the beam would also diffract.

Authors: Our purpose was not to characterize the exact orientation of the crystal planes with respect to the crystal faces. Rather, it was to perform a preliminary study on a number of different aspects of a CPC system. We attempted to determine an approximate orientation. This can be accomplished by looking at the prevalent diffracting planes with respect to crystal orientation. One can also say that crystal planes at an angle to the incident beam will diffract less well than those parallel to the incident beam and this fits the data and our present interpretation.

M. Iijima: Is the chemical formula for HAp correct? HAp has a fixed composition, $\text{Ca}_{10}(\text{PO}_4)_6(\text{OH})_2$. The stoichiometry of HAp strongly depends on the method of synthesis. It is difficult to obtain HAp with a Ca/P = 1.67. That is why "HAp" sometimes does not show the characteristic Ca/P of 1.67. However, this does not mean that HAp does not have a fixed composition.

Authors: The chemical formula for HAp ($\text{Ca}_{10-x}(\text{HPO}_4)_x(\text{PO}_4)_{6-x}(\text{OH})_{2-x}$) is correct. Regardless of whether or not one believes that thermodynamically stable HAp of variable composition exists, it has been shown in the literature by a large number of researchers that variable composition apatite will form with the compositional relationship shown above. We have established thermodynamically stable HAp that can have more than a single composition. The Ca/P of stable HAp will decrease with decreasing pH. Reactions in the

CPC system support this. We have shown in numerous previous works that CPC reactions between DCP (CaHPO_4) and TetCP having a bulk Ca/P ratio of 1.5 react to completion. In these reactions, the TetCP is consumed prior to the DCP indicating that the initial HAp that forms has a Ca/P > 1.5. In the absence of the formation of a thermodynamically stable calcium deficient hydroxyapatite, there would be absolutely no driving force for further reaction. In that instance, the remaining DCP and the HAp initially formed should approach an invariant condition. This does not occur; rather, the previously formed HAp reacts with the remaining DCP to form HAp with a Ca/P of ~ 1.5 . There is a large number of materials known to have variable compositions that are all thermodynamically stable. A number of different oxides show this characteristic (TiO_{2-x} , ZrO_{2-x} , $\text{Fe}_2\text{O}_{3-x}$, etc.; Levin and McMurdie, 1975; Levin *et al.*, 1964). While these are oxides, they are analogous to HAp. The stable compositions of these materials are functions of the activity of O_2 . Thus, there is a functional relationship between composition and activity. The functional relationship in the HAp system is between composition and the activity of H^+ . The activity or concentration of H^+ (pH) affects the concentration/activity of the different phosphate species in solution and thus the amount of HPO_4^{2-} thermodynamically stable in the apatite structure. Another material that has been shown to exhibit anomalous behavior is calcium silicate hydrate. This material has reproducible solubility curves and been shown to have stable compositions with CaO/SiO_2 molar ratios of 0.833 to 1.7 (Taylor, 1990).

M. Iijima: When NCP formed and remained after reaction, are the chemical equations shown in Reactions 1 and 2 correct? The formula might change depending on the quantity of NCP and the reaction temperature.

Authors: Rigorously, your comment is correct. It should be emphasized though, that the quantity of this NCP phase was quite small in relation to the total amount of crystalline HAp observed, and this phase is metastable and reacts over time to form a crystalline HAp. Reactions 1 and 2 show the reactants going to the final products. These equations were not intended to show the mechanistic reaction path in detail. Our calorimetric study on these CPCs suggest that the quantity of NCP formed as an intermediate is approximately constant over the temperature range investigated (TenHuisen and Brown, 1996). It is not possible to quantify how much intermediate NCP forms due to the variable composition of HAp, the amorphous character of the NCP, and multiple reactions occurring simultaneously.

M. Iijima: How long did it take to complete each

reaction?

Authors: A detailed discussion on the kinetics of these reactions has recently been published (TenHuisen and Brown, 1996). The rate of reaction was shown to exhibit a high thermal dependence over the temperature range investigated ($15\text{-}70^\circ\text{C}$) with complete reaction being reached between 0.5 and 35 hours.

M. Iijima: Was the TEM observation performed with a cool stage? If not, was it possible that the amorphous electron diffraction pattern was caused by beam damage?

Authors: TEM analysis did not use a cooled stage. We did see beam damage when the beam was concentrated, that is at very high magnifications or during EDS acquisitions. Therefore, the beam was kept very diffuse; this resulted in no observable damage to the particles.

M. Iijima: The increase in surface area with the decrease in temperature was explained by the pH dependence of SHAp formation. It is not clear to me how the pH dependence supported the present observation? Did the temperature affect surface area in the same manner as solution pH did? If so, please explain.

Authors: As the temperature decreases, the effects of solution conditions on the surface area (due to nucleation and growth rates) increase due to slower kinetics. SHAp formation occurs at higher pH values than does CDHAp for reactions between DCPD and TetCP (TenHuisen and Brown, 1997). As the reaction temperature decreases, the pH value at any given stage of these reactions increases. Since the ion concentrations measured in solution during these formation reactions were of the same order of magnitude for both CDHAp and SHAp, and the solubility of HAp is lower at higher pH values, the driving force for precipitation should be greater for the SHAp system due to the elevated pH. This in turn would produce a higher nucleation density and ultimately a larger surface area. We always observed greater surface areas for SHAp than for CDHAp at temperatures where there were differences in the kinetics ($< 55^\circ\text{C}$). Therefore, in a way, the temperature affected the surface area in the same manner as the solution pH.

M. Iijima: The authors concluded that the relative rates of nucleation versus growth of CDHAp decreased with decreasing temperature (below approximately physiologic) while that of the SHAp was constant; this is rather confusing. Is there any data of the temperature dependence of the nucleation and growth rates of SHAp and CDHAp?

M. Markovic: Do you have any experimental data on rate of nucleation and crystal growth in the DCPD/TetCP/water system?

Authors: For surface area to remain constant as the temperature is changed (SHAp below physiologic), the rate at which nucleation occurs in relation to the rate at which growth occurs must remain approximately constant. Since the actual rate of both are decreasing with decreasing temperature, as reflected in slower kinetics, the ratio of the two must be approximately constant to result in a similar surface area. This also explains the observations made in the CDHAp (below approximately physiologic) in that the decrease in the rate of growth must be occurring more slowly than the decrease in the rate of nucleation to result in a larger particle size (smaller surface area) with the lowering of reaction temperature. These arguments are of course simplistic in that multiple reactions are occurring simultaneously. There is a fair amount of literature discussing the rates of nucleation and growth of apatites in much more dilute systems. We do not feel that previous results can be extrapolated to our system for this reason and due to the fact that these other systems have extraneous cationic and anionic species present, all of which influence speciation, driving force, etc.

M. Iijima: With regard to diffraction, there is no 002 diffraction plane in a crystal. Note that the 002 reflection is caused by the secondary diffraction of a 001 plane, not by a 002 plane.

Authors: There is a (002) in hydroxyapatite. The (002) refers to the plane of atoms in a crystal that crosses the c-axis at 0,0,1/2. This is an entirely different plane of atoms than those corresponding to the (001). The presence of an (002) results in a new diffraction condition, thus resulting in the presence of a new diffraction peak.

M. Iijima: How was the change in the connectivity of the CPC with temperature explained?

Authors: The interparticulate connectivity increased with decreasing temperature. This is related to the changes in the reaction kinetics, rate of nucleation, rate of growth, and solubility properties of the apatite. As temperature is increased the solubility of HAp decreases (i.e., it is retrograde). This, combined with the epitaxial relationship between TetCP and HAp, result in more HAp formation on or near the TetCP particulate surfaces. The greater degree of TetCP overgrowth at lower temperatures is supported by lower pH values during any stage of the reaction (TenHuisen and Brown, 1997) and the presence of more donut or shell structures.

M. Iijima: Did the difference in surface area with temperature correlate with that in interparticulate connectivity?

Authors: In general, the interparticulate connectivity in-

creased as the surface area decreased. Finer microstructural features appeared to favor bonding between the initial TetCP particles.

M. Iijima: Which factor had a greater effect on the surface area, the quantity of NCP or microstructure and size of apatite?

Authors: The surface area was most definitely affected by changes in the microstructural features of the apatite. We need to emphasize that, while we discussed the presence of NCP in our samples in great detail, upon reaching complete reaction, the quantity of it in our samples was quite small in comparison to the quantity of apatite.

P. Li: There is no evidence supporting that one apatite is Ca-deficient, and another is stoichiometric. On the contrary, the results of the paper indicate that both apatites are non-stoichiometric. This is consistent with the observation that a non-crystalline calcium phosphate (NCP) exists with an apatite phase in the mixture. Hence, the Ca/P ratio of the formed apatite could not be determined unless the quantity and the Ca/P ratio of the NCP are known.

M. Markovic: The name stoichiometric hydroxyapatite (SHAp) for the precipitate resulting from the initial reactant mixture with a Ca/P = 1.67 could be misleading, implying that its Ca/P ratio is 1.67. The majority of HAp previously synthesized under similar conditions contained HPO₄ ions and therefore Ca/Ps < 1.67.

Authors: These apatites were synthesized at a liquid-to-solids ratio of 1-to-1 (v/w). The solubility of HAp is low, resulting in a liquid with a low ionic strength. Therefore, if the bulk stoichiometry of the cement reactants results in a Ca/P molar ratio of 1.67, and the reaction consumes all of these calcium phosphate reactants, the final apatitic product must have a Ca/P molar ratio very close to 1.67. If the apatite were significantly calcium-deficient, mass balance dictates that a phase with a Ca/P ratio greater than 1.67 also exists. All of our reactions reach completion as indicated by X-ray diffraction analysis, which has a sensitivity of ~2% by weight. The quantity of NCP present is quite small; its presence was used to explain the formation of an intermediate amorphous calcium phosphate phase. The SHAp may have a small amount of HPO₄ ions present in the structure, but the Ca/P ratio of the final apatite must be extremely close to the bulk. For this reason, we call the product from this reaction SHAp. Although any HAp with a Ca/P < 1.67 is referred to as calcium-deficient, in this study we have defined a specific Ca/P ratio (1.5) for calcium-deficient HAp (CDHAp).

P. Li: As indicated in the paper, NCP serves as an intermediate phase during the apatite formation. The

authors try to relate the surface area of the reacted products to the rates of hydroxyapatite nucleation and growth. The reviewer feels such relation is arbitrary.

Authors: We know that NCP forms as an intermediate phase in the formation of our apatites. It is well documented in the literature that this phase can form first during the precipitation of HAp (depending on solution conditions). It has also been extensively published that this phase transforms within a matter of hours into apatite in the absence of other extraneous ions such as Mg, P_2O_7 , citrate, etc. Although we observed this intermediate phase, its quantity is small in relation to the apatite. It would not have been observable if we had let the samples react for slightly longer times. Although NCP forms as an intermediate in our reactions, calorimetrically, its quantity is constant for a given bulk stoichiometry (TenHuisen and Brown, 1996). The amount of NCP that forms as an intermediate is a function of the bulk stoichiometry, but is not affected by the reaction temperatures investigated. This has been previously published and referenced in the present manuscript (Martin and Brown, 1995; TenHuisen and Brown, 1997). Therefore, our discussion on the relative rates of nucleation versus growth of the final apatitic product holds true.

P. Li: The discussion on the kinetics of apatite formation is not convincing because it is merely based on SEM/TEM observation.

Authors: The kinetics of these reactions have been thoroughly discussed in our prior publications. It has been shown both by calorimetry (TenHuisen and Brown, 1996) and by X-ray diffraction studies (TenHuisen and Brown, 1997) that the basic calcium phosphate reactant, TetCP, is consumed prior to the acidic reactant, DCPD, in our systems. This was extensively discussed and referenced throughout this manuscript. Indeed, the micrographs presented in this work support our previous findings.

M. Markovic: What was the particle size of the DCPD?

Authors: We did not measure or report a particle size for the DCPD used in this study. The morphology of the DCPD used in this study consists of extremely thin plates (~ 5 - $10 \mu\text{m}$ across and $< 0.1 \mu\text{m}$ thick). After intergrinding the DCPD with the TetCP, the DCPD particles are drastically reduced in size due to their relative softness.

Reviewer VII: The authors believe that NCP first formed in the course of cementing reaction and then transformed to hydroxyapatite. However, the authors also use the concept of nucleation/growth of hydroxyapatite and their relation to solution chemistry to interpret their observation. The authors should clarify

how nucleation and growth rates of hydroxyapatite correlate to the solution chemistry if hydroxyapatite is transformed from NCP. The authors try to explain their data with the relation of nucleation of hydroxyapatite to the supersaturation degree. Such explanation is not convincing because the growth rate of hydroxyapatite also increases with supersaturation degree. Therefore, it is hard to determine the relationship between the supersaturation degree and the nucleation/growth rate, a determinant of surface area.

Authors: We see no inconsistency here. It must be remembered that HAp and NCP formation are competitive. Thus, both can form together. However, the NCP which does form eventually converts to HAp.

Reviewer VII: There is no scientific evidence to support the relationship between the NCP proportion and the reaction temperature. The statement that "the proportion of NCP was observed to increase with decreasing temperature and was more prevalent in CDHAp" is not well supported because: (1) TEM analysis is not quantitative study; (2) TEM gives very local information; and (3) the resultant products are not uniform in terms of morphology and perhaps the chemical composition.

Authors: We believe the microstructural features discussed in the paper to be representative.

Reviewer VII: There is no argument that cementing reaction and resultant product largely depend on the size of calcium and phosphate particles, their relative amount, temperature and the type and amount of the solution. This means that morphology of apatite is related to the particle size of DCPD and TetCP particles. Therefore, the particle size of DCPD should be analyzed and included in your report.

Authors: This is true; we only studied one size so it is not possible to make such an argument. However, the reviewer's suggestion that HAp morphology is related to the particle size of the reactants is an assumption. The ultrastructure of the HAp is unaffected. On the meso-scale, there is a relationship between the pore structure and overall microstructure which is related to the amount of water and the particle sizes of the reactants. We have discussed these aspects in earlier publications {Fulmer M, Brown PW (1991) The Kinetics of hydroxyapatite formation at low temperature. *J Am Ceram Soc* 74: 934-940; and Brown PW, Hocker N, Hoyle S (1991) The solution chemistry of hydroxyapatite formation at low temperature. *J Am Ceram Soc* 74: 1848-1855).